

CT Breast Dose Reduction with the Use of Breast Positioning and Organ-Based Tube

Current Modulation

by

Wanyi Fu

Department of Electrical and Computer Engineering
Duke University

Date: _____

Approved:

Ehsan Samei, Supervisor

Loren W. Nolte, Chair

Joseph Yuan-Chieh Lo

Thesis submitted in partial fulfillment of the
requirements for the degree of Master of
Science in the Department of
Electrical and Computer Engineering in the
Graduate School of Duke University

2016

ABSTRACT

CT Breast Dose Reduction with the Use of Breast Positioning and Organ-Based Tube

Current Modulation

by

Wanyi Fu

Department of Electrical and Computer Engineering
Duke University

Date: _____

Approved:

Ehsan Samei, Supervisor

Loren W. Nolte, Chair

Joseph Yuan-Chieh Lo

An abstract of a thesis submitted in partial
fulfillment of the requirements for the degree
of Master of Science in the Department of
Electrical and Computer Engineering in the Graduate School of
Duke University

2016

Copyright by
Wanyi Fu
2016

Abstract

Purpose: The purpose of this work was to investigate the breast dose saving potential of a breast positioning technique (BP) for thoracic CT examinations with organ-based tube current modulation (OTCM).

Methods: The study included 13 female patient models (XCAT, age range: 27-65 y.o., weight range: 52 to 105.8 kg). Each model was modified to simulate three breast sizes in standard supine geometry. The modeled breasts were further deformed, emulating a BP that would constrain the breasts within 120° anterior tube current (mA) reduction zone. The tube current value of the CT examination was modeled using an attenuation-based program, which reduces the radiation dose to 20% in the anterior region with a corresponding increase to the posterior region. A validated Monte Carlo program was used to estimate organ doses with a typical clinical system (SOMATOM Definition Flash, Siemens Healthcare). The simulated organ doses and organ doses normalized by $CTDI_{vol}$ were compared between attenuation-based tube current modulation (ATCM), OTCM, and OTCM with BP (OTCM_{BP}).

Results: On average, compared to ATCM, OTCM reduced the breast dose by 19.3±4.5%, whereas OTCM_{BP} reduced breast dose by 36.6±6.9% (an additional 21.3±7.3%). The dose saving of OTCM_{BP} was more significant for larger breasts (on average 32, 38, and 44%

reduction for 0.5, 1.5, and 2.5 kg breasts, respectively). Compared to ATCM, OTCM_{BP} also reduced thymus and heart dose by $12.1 \pm 6.3\%$ and $13.1 \pm 5.4\%$, respectively.

Conclusions: In thoracic CT examinations, OTCM with a breast positioning technique can markedly reduce unnecessary exposure to the radiosensitive organs in the anterior chest wall, specifically breast tissue. The breast dose reduction is more notable for women with larger breasts.

Contents

Abstract	iv
List of Tables	viii
List of Figures	ix
Acknowledgements	xi
1. Introduction	1
2. Materials and Methods	3
2.1 Computational phantoms	3
2.2 Morphing Breast.....	5
2.3 CT examination Simulations	7
2.4 Tube Current Profiles	7
2.5 Organ Dose Estimation	10
3. Results	13
3.1 breasts dose	13
3.2 Other organ dose.....	18
4. Discussion	25
4.1 Organ-based tube current modulation and dose.....	25
4.2 Compare with literature.....	26
4.2.1 Breast modeling.....	26
4.2.2 Dose savings.....	27

4.3 Breast positioning technique advantage	30
4.5 Limitations.....	30
5. Conclusion.....	32
References	33

List of Tables

Table 1: Mean of percentage of breast volume from all phantoms within $\pm 60^\circ$ frontal zone.....	6
Table 2: CTDI _{vol} value used for each phantom and scan	10
Table 3: Average CTDI _{vol} -normalized-breast dose coefficients and difference from ATCM, OTCM, and OTCMBP	15
Table 4: Average value of CTDI _{vol} -normalized-breast dose coefficients and difference in different sized breast	16
Table 5: Fitting coefficients of breast dose fitted vs. breast mass.	18
Table 6: Fitting parameters of organ dose v.s. chest diameter	23

List of Figures

Figure 1: The BMI and age distribution of the computational phantoms	3
Figure 2: The three-dimensional frontal view of phantoms.	4
Figure 3: Transverse slice of a modified voxelized XCAT phantom. Three breast sizes are shown: (a) small, (b) medium (c) large and the corresponding slice with breast position altered while volume is constant (d), (e), (f) respectively. The breast tissue is highlighted in red.	6
Figure 4: An example of the tube current profile generated for attenuation based tube current modulation (ATCM), organ-based tube current modulation (OTCM), and OTCM with breast positioning for a phantom. The shaded regions correspond to the dose reduction zone.	9
Figure 5: a) Average of $CTDI_{vol}$ -normalized-breast dose coefficients and b) breast dose simulated with ATCM, OTCM, and OTCMBP for all phantoms with 50/50 and 20/80 breasts. Error bars represent ± 1 standard deviation.	14
Figure 6: Dose distribution plots of three example patients with small (a), medium (b), and large (c) breasts.	14
Figure 7: $CTDI_{vol}$ -normalized-breast dose coefficients linearly fitted to breast mass scanned with ATCM, OTCM and OTCM _{BP} as equation (2).	17
Figure 8: Differentiation for a) $CTDI_{vol}$ -normalized-breast dose coefficients and b) breast dose across ATCM, OTCM and OTCM _{BP}	20
Figure 9: A) $CTDI_{vol}$ -normalized-organ dose and B) organ dose fitted against model chest diameter as equation (1). Example organs from anterior (a), (b), and (c), medial and distributed (d) and (e), and posterior (f) group.	22
Figure 10: a) $CTDI_{vol}$ -normalized-breast dose coefficients and b) breast dose linearly fitted to breast mass scanned with ATCM, OTCM and OTCM _{BP} as equation (2).	28
Figure 11: Skin dose from ATCM and OTCM in computerized phantom for this study compared with Duan <i>et al.</i> measured with physical phantoms with OTCM and fixed mA. The dose was averaged to a unit mean for comparisons. For this study, skin dose	

profile was averaged across all phantoms. The dose reduction zone is shaded in yellow.
.....29

Acknowledgements

The author would like to thank Xiaoyu Tian, Gregory Sturgeon, Greeshma Agathya and W. Paul Segars from Duke University, Mitchell M. Goodsitt and Ella A. Kazerooni from University of Michigan, and Juan Carlos Ramirez Giraldo from Siemens Health Care for their valuable discussions.

1. Introduction

Computed tomography (CT) has significantly benefitted the clinical diagnosis of a wide spectrum of diseases. In the past decades, the use of CT has grown exponentially. In 2014, approximately 81.2 million CT examinations were performed in the United States^{1, 2}. The increased number of CT examinations has led to concerns about the associated population-based radiation dose³. Significant efforts have been made to minimize unnecessary radiation exposure and maximize patient benefits through the development of dose reduction techniques⁴. These techniques generally aim to reduce the unnecessary exposure to major radiosensitive organs while maintaining the required image quality level^{5, 6}.

Breasts are among the most radiosensitive organs for female patients^{7,8}. In thoracic CT examination, although breasts are usually not diagnostically targeted, they receive a considerable amount of radiation dose⁹⁻¹². In an effort to protect superficial radiosensitive organs such as breasts, some vendors have developed organ based tube current modulation (OTCM) techniques¹³. In one implementation of OTCM, the tube current (mA) is reduced by 80% in the anterior region ($\pm 60^\circ$) of the patient with a corresponding increase in the posterior region (X-CARE, Siemens Healthcare). It has been reported that, with OTCM, breast doses can be reduced by 30-50% with no detrimental effect on image quality^{5, 6, 14}. However, a major challenge associated with the

OTCM technique has been the extension of the breasts to outside the dose reduction zone¹⁵. A previous study has shown that, without any constraint, when the patient is supine, the breast tissue extends within an average angular zone for 155°; this is larger than the 120° dose reduction zone angle¹⁶. In effect, for most women, at least one breast partly resides in the increased dose zone, between $\pm 75^\circ$ and $\pm 84^\circ$ ¹⁷. Another challenge with OTCM and associated breast dose is that the outer breast region contains a higher percentage of glandular tissue, making it more susceptible to cancer¹⁸. More than half of breast malignant tumors first develop in the upper outer quadrant of the breast¹⁹. As a result, the effectiveness of OTCM has been questioned, especially for women with larger breasts¹⁵.

The purpose of this study was to evaluate the dose reduction potential of a specially-designed breast positioning technique for OTCM examinations. The breast positioning technique was modeled by constraining most of the breast tissue to within the dose reduction zone. The dose reduction potential of this technique was evaluated across a library of phantoms with various ages, weights, and breast sizes. The organ doses were normalized by $CTDI_{vol}$ and compared from Monte Carlo simulations with three CT scan protocols: attenuation based tube current modulation (ATCM), OTCM, and OTCM with breast positioning altered (referred to as OTCM_{BP}).

2. Materials and Methods

2.1 Computational phantoms

This study included models of thirteen female adult patients (age range: 27-65 y.o., weight range: 52 to 105.8 kg) who received a chest and abdominal-pelvis, or a chest-abdominal-pelvis CT examination at our institution. The patients represented the anatomical variability amongst a clinical population with a broad range of age and BMI distribution (Figure 1).

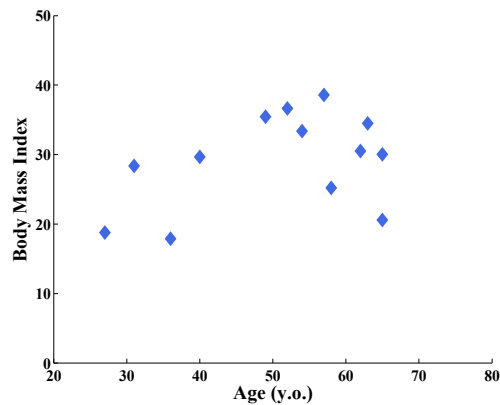


Figure 1: The BMI and age distribution of the computational phantoms

The models have been developed from the CT images of the patients²⁰. Initially, large organs within the scan volumes were segmented to generate phantom masks followed by 3D triangulated polygon models using a marching cubes algorithm. The polygon structure was translated to 3D non-uniform rational B-spline surface (NURBS) (Rhinceros, McNeel North America, Seattle, WA). The remaining organs and structures were generated by morphing a template's corresponding anatomies. The template was

segmented from high-resolution visible human female full-body images^{21, 22}. The organ volume was rescaled to the organ volume and anthropometry data reported in ICRP 89²³. The computer modeled frontal views are shown in Figure 2. Each phantom was voxelized at isotropic resolution of 3.45 mm for input into a Monte Carlo simulation program. The resolution was chosen considering the anatomic details and simulation time²⁴.

To investigate the effect of dose on glandular density, two compositions of breasts were simulated: (1) 50/50 breast (50% glandular tissue and 50% adipose tissue), as a representative case for younger women and (2) 20/80 breast (20% of glandular tissue and 80% adipose tissue), which was an approximation of mean glandular percentage in a wide population²⁵⁻²⁷.

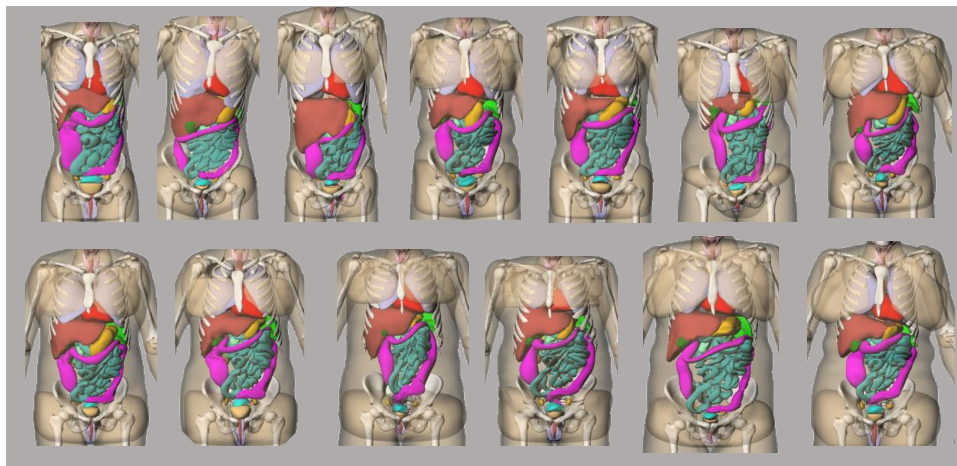


Figure 2: The three-dimensional frontal view of phantoms.

2.2 Morphing Breast

The phantom library was enhanced by modeling each phantom with two additional breast sizes (Figure 3). To allow for the use of additional breast sizes, the torso surface of each phantom was first modeled as a smooth breast-free surface. The individual breasts were modeled as closed surfaces that were added to the breast-free surface. The modeling of two additional breast geometries per patient providing a library of 39 phantoms preserved the breast-free surface and kept all other organs and structures constant.

The breast deformation to desired positioning was solved using finite element method (FEBio, University of Utah's Musculoskeletal Research Laboratories and Columbia's Musculoskeletal Biomechanics Laboratory)²⁸. The breasts were voxelized at a resolution of 0.2 mm to create hexahedral finite elements. The breast elements were morphed by a body force in up and towards the midline of the torso direction with experimentally determined magnitude. The breast elements adjacent to the body were constrained to have zero displacement. The breasts were further checked and scaled manually to ensure the breast volume remained constant and the targeted positioning was achieved. Figure 3 shows an example phantom with three breast sizes before and after applying BP. The phantom library was further divided into three groups by breast size: small (447 ± 187 g), medium (1068 ± 222 g), and large-sized (1929 ± 432 g) groups.

The percentage of breast volume within dose reduction zone in standard supine positioning and after applying BP is listed in Table 1.

Table 1: Mean of percentage of breast volume from all phantoms within $\pm 60^\circ$ frontal zone

	Without BP (%)	With BP (%)	Change in Volume (%)
Small breasts	68.5 ± 11.1	93.9 ± 4.2	25.5 ± 12.1
Median breasts	68.0 ± 17.0	93.7 ± 5.2	25.6 ± 14.3
Large breasts	57.2 ± 14.5	93.9 ± 3.3	36.6 ± 12.3
All Models	64.6 ± 15.2	93.8 ± 4.0	29.1 ± 14.1

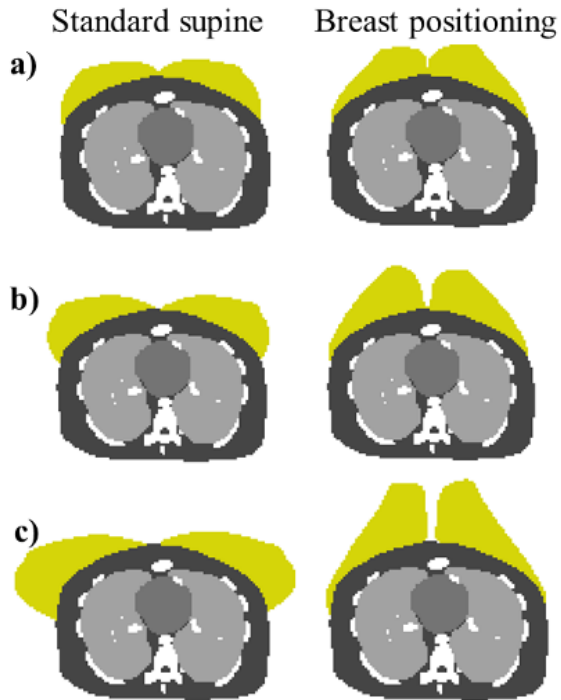


Figure 3: Transverse slice of a modified voxelized XCAT phantom. Three breast sizes are shown: (a) small, (b) medium (c) large and the corresponding slice with breast position altered while volume is constant (d), (e), (f) respectively. The breast tissue is highlighted in red.

2.3 CT examination Simulations

A previously validated Monte Carlo simulation program was used to simulate CT scans^{27, 29}. The package included PENLOPE as a subprogram to track the energy loss of photons and electrons^{30, 31}.

A 128-section CT system (SOMATOM Definition Flash; Siemens Healthcare, Forchheim, Germany) was modeled^{32, 33}. The scanner parameters were 120 kVp, pitch factor of 0.6, rotation time of 0.5 s, table speed of 2.304 cm/rot, 38.4 mm collimation, and CTDI_{vol} value denoted below. A clinical chest CT examination was simulated for each phantom. The scan coverage was defined as 1 cm above lung apex to 1 cm below the lung base.

2.4 Tube Current Profiles

The attenuation-based tube current modulation profile (mA_{ATCM}) simulated the virtual CAREdose4D, which takes into account attenuation of patient in both longitudinal (Z) and angular (XY) plane³⁴. The XYZ attenuation through the phantom was simulated by a previously developed ray-tracing program²⁴. In brief, at each projection angle θ , the 'fanbeam' function was used to measure the line integrals of attenuation coefficients along each ray from the source to each detector bin (Matlab2010a; Mathworks, Natick, MA). The maximum line integrals of attenuation coefficients (ud)

from all detector bins at θ was selected as the basis to generate tube current profile at θ .

The tube current profile was modeled as³³

$$mA_{ATCM}(\theta) = mA_0 e^{\alpha*(-ud(\theta))}, \quad (1)$$

where mA_0 and $mA_{ATCM}(\theta)$ are the fixed and attenuation modulated mA, respectively, $ud(\theta)$ is the maximum line integrals of attenuation coefficients calculated at θ , and α is the modulation strength²⁴. A typical averaged modulation strength level ($\alpha=0.5$) was used. Finally, at each rotation angle, the tube current was scaled to below the systems' maximum mA limit²⁴.

To generate the organ based tube current profile (mA_{OTCM}), X-CARE was simulated (X-CARE, Siemens Healthcare). First, the longitudinal (Z-plane) profile was reduced to 80% between $\pm 60^\circ$ of each patient and the reduction was evenly divided and added to the remaining projections within one rotation. The angular (XY-plane) modulation was turned off¹³. The longitudinal-profile was modeled as²⁴

$$mA_Z(\theta) = 0.5(mA_0 e^{\alpha*(ud(\theta_{AP}))} + mA_0 e^{\alpha*(ud(\theta_{LAT}))}), \quad (2)$$

where mA_0 and $mA_Z(\theta)$ are the fixed and longitudinal modulated mA, and $ud(\theta_{AP})$ and $ud(\theta_{LAT})$ are the attenuation in AP (anterior-posterior) and in LAT (lateral) direction along the Z-plane at gantry angle θ . This approach emulated the CT system, in that the Z-profile was generated prior to the scan based on localization radiographs in LAT and

AP directions. The simulation further modeled gradual change in mA (slope as a function of rotation time, upward and downward transition time) when switching between mA reduction and mA increase zone. Using 0.28 rot/s and 1 rot/s per Duan *et al.*¹³, the mA upward and downward times at 0.5 rot/s was estimated using linear approximation as 17% and 6% of rotation time, respectively. The mA value was generated for models with and without BP separately, mA_{OTCM} and $mA_{OTCM,BP}$, respectively. The mA_{ATCM} , mA_{OTCM} , and $mA_{OTCM,BP}$ of one example phantom is shown in Figure 4.

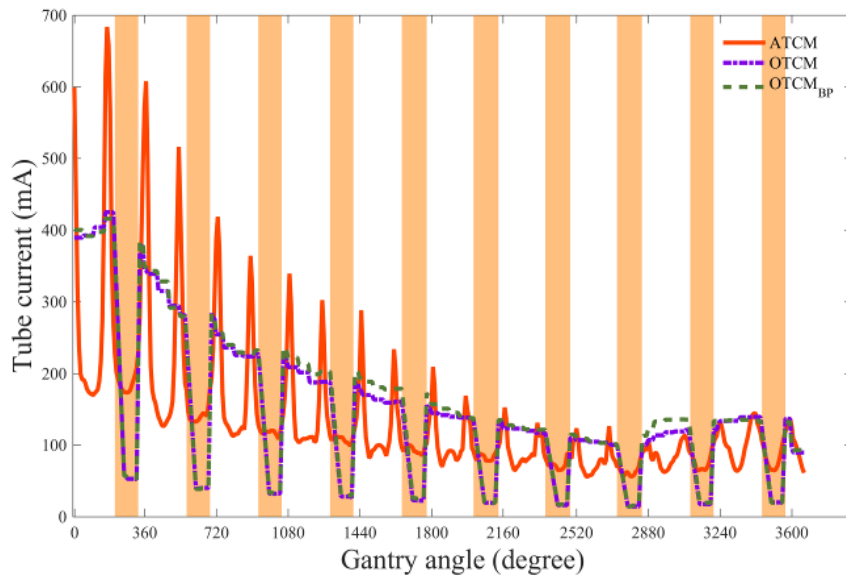


Figure 4: An example of the tube current profile generated for attenuation based tube current modulation (ATCM), organ-based tube current modulation (OTCM), and OTCM with breast positioning for a phantom. The shaded regions correspond to the dose reduction zone.

2.5 Organ Dose Estimation

Organ doses were determined by tracking the energy deposited within each organ using flux for a particular $CTDI_{vol}$ value. The reference $CTDI_{vol}$ of 14.1 mGy was used for quality reference mAs of 150. The $CTDI_{vol}$ values were adjusted as dictated by the applied TCM. Table 2 summarized the corresponding $CTDI_{vol}$ value. The organ doses were further normalized by $CTDI_{vol}$ to derive the $CTDI_{vol}$ -to-organ dose conversion coefficients (h factor) so that the results can be potentially generalized to other scanners and protocols³⁵. Furthermore, expanding the results in terms of $CTDI_{vol}$ normalized dose value could be interpolated as comparing technique where total flux (and thus image quality by implication) remain constant. The breast dose was computed for both 50/50 and 20/80 breasts assume breast tissue to be uniform. A side study indicated that average glandular dose (AGD) is very similar to uniform tissue dose results.

Table 2: $CTDI_{vol}$ value used for each phantom and scan

	1st size		2nd size		3rd size	
	ATCM/ OTCM	OTCMBP	ATCM/ OTCM	OTCMBP	ATCM/ OTCM	OTCMBP
phantom 1	6.8	6.8	6.9	6.8	7.0	7.1
phantom 2	8.8	8.5	9.1	8.8	10.2	9.2
phantom 3	4.7	4.5	4.8	4.7	4.9	4.8
phantom 4	12.7	12.5	13.3	12.5	15.4	13.3
phantom 5	7.0	7.0	7.3	7.1	8.3	7.3
phantom 6	11.8	11.2	13.7	12.8	12.8	11.9
phantom 7	7.6	7.3	7.8	7.7	8.7	7.8

phantom 8	14.3	14.5	14.6	15.1	16.2	17.1
phantom 9	8.6	8.2	9.2	9.1	10.4	10.2
phantom 10	5.5	5.5	5.6	5.6	6.0	5.7
phantom 11	8.6	8.4	8.7	8.4	10.3	9.6
phantom 12	12.0	12.4	12.6	12.7	13.6	11.7
phantom 13	9.9	9.8	11.0	10.3	12.5	10.9

To investigate the effect of $OTCM_{BP}$ on breast dose, dose percentage difference was measured between $OTCM$ and $OTCM_{BP}$. The effect of BP on the difference between organ-based and attenuation-based tube current modulation was then compared. The dose percentage difference was calculated for $OTCM$, $OTCM_{BP}$ and $ATCM$, respectively. Organs were further grouped into anterior organs, medial or distributed organs, and posterior organs based on organ geometric center locations with respect to the CT scanner.

Because breast positioning repositions more breasts volume within the dose reduction zone for larger breasts (Table 1), to assess the effect of breast mass on dose reduction potential, the $CTDI_{vol}$ -normalized-breast dose coefficients and the breast dose value were further fitted to breast mass as

$$\hat{h}_{breast} = p_{h,1}m_{breast} + p_{h,2}, \quad (3a)$$

$$\hat{D}_{breast} = p_{D,1}m_{breast} + p_{D,2}, \quad (3b)$$

where h_{breast} and D_{breast} denote the CTDI_{vol}-to-breast dose conversion coefficient and breast dose, respectively, m_{breast} is the weight of both breasts in each phantom, and p_1 and p_2 are the linear fitting coefficients.

3. Results

3.1 breasts dose

On average, compared to ATCM, OTCM reduced the $CTDI_{vol}$ -normalized-50/50 breast dose by $19.3 \pm 4.5\%$. The $CTDI_{vol}$ -normalized average breast dose was further decreased by an additional $-21.3 \pm 7.3\%$ to $-36.6 \pm 6.9\%$ with $OTCM_{BP}$ compared to ATCM (Figure 5). The corresponding values in terms of breast dose were $24.1 \pm 9.7\%$ ($OTCM_{BP}$ to OTCM) and $38.8 \pm 8.4\%$ ($OTCM_{BP}$ to ATCM), respectively. Table 3 shows the average $CTDI_{vol}$ -normalized-breast dose coefficients and the breast dose values for the 50/50 and 20/80 breasts simulated with ATCM, OTCM and $OTCM_{BP}$. The difference in $CTDI_{vol}$ -normalized-breast-dose between the two breast compositions was $8.9 \pm 0.6\%$, but the two compositions exhibited very similar trends in terms of impact of imaging method on dose. Figure 6 shows dose distribution plots of one phantom with small, medium, and large breasts undergoing ATCM, OTCM, and $OTCM_{BP}$ exams at a mid-transverse plane.

The breast dose saving of $OTCM_{BP}$ compared to ATCM was more significant for patients with larger breasts. For small (447 ± 187 g), medium (1068 ± 222 g), and large-sized (1929 ± 432 g) groups, the $OTCM_{BP}$ and ATCM h factors difference were $-31.4 \pm 6.5\%$, $-36.8 \pm 5.0\%$, and $-41.5 \pm 5.4\%$. The corresponding values in terms of breast dose were $32.6 \pm 7.0\%$, $38.3 \pm 5.2\%$, and $45.4 \pm 7.7\%$, respectively (Table 4). Compared to

OTCM alone, $OTCM_{BP}$ h factors decreased by $17.3 \pm 7.8\%$, $20.4 \pm 6.2\%$, and $26.3 \pm 5.0\%$ for small, medium, and large sized groups, respectively. The corresponding value in terms of breast dose were $18.7 \pm 9.0\%$, $22.3 \pm 7.1\%$, and $31.3 \pm 8.7\%$, respectively. The fitting coefficients of dose values vs. breast mass for the three protocols are given in Table 5 (Figure 7).

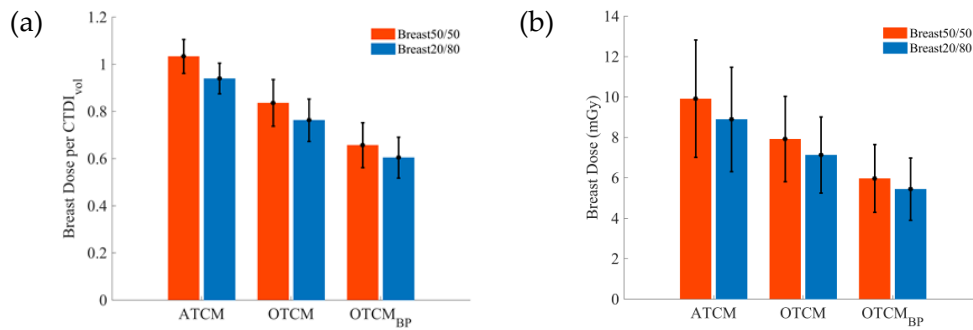


Figure 5: a) Average of CTDI_{vol}-normalized-breast breast dose coefficients and b) breast dose simulated with ATCM, OTCM, and OTCMBP for all phantoms with 50/50 and 20/80 breasts. Error bars represent ±1 standard deviation.

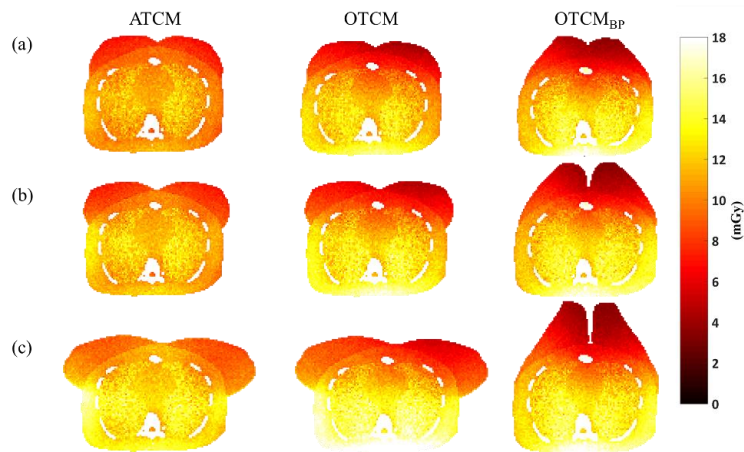


Figure 6: Dose distribution plots of three example patients with small (a), medium (b), and large (c) breasts.

Table 3: Average CTDI_{vol}-normalized-breast dose coefficients and difference from ATCM, OTCM, and OTCMBP

CTDI_{vol}-normalized-breast dose coefficients						
Breast Composition	ATCM Dose per CTDI _{vol}	OTCM Dose per CTDI _{vol}	OTCM _{BP} Dose per CTDI _{vol}	OTCM _{BP} to ATCM difference (%)	OTCM to ATCM difference (%)	OTCM _{BP} to OTCM difference (%)
50/50	1.0 ± 0.1	0.8 ± 0.1	0.7 ± 0.1	-36.6 ± 6.9*	-19.3 ± 4.5*	-21.3 ± 7.3*
20/80	0.9 ± 0.1	0.8 ± 0.1	0.6 ± 0.1	-35.8 ± 6.9*	-19.1 ± 4.5*	-20.7 ± 7.2*
Breast dose						
Breast Composition	ATCM Dose (mGy)	OTCM Dose (mGy)	OTCM _{BP} Dose (mGy)	OTCM _{BP} to ATCM difference (%)	OTCM to ATCM difference (%)	OTCM _{BP} to OTCM difference (%)
50/50	9.9 ± 2.9	7.9 ± 2.1	6.0 ± 1.7	-38.8 ± 8.4*	-19.3 ± 4.5*	-24.1 ± 9.7*
20/80	8.9 ± 2.6	7.1 ± 1.9	5.4 ± 1.5	-37.9 ± 8.3*	-19.1 ± 4.5*	-23.2 ± 9.5*

¹Negative means dose reduction.

* represents statistical significant.

Table 4: Average value of CTDI_{vol}-normalized-breast dose coefficients and difference in different sized breast group.

CTDI_{vol}-normalized-breast dose coefficients						
Breast Size	ATCM Dose per CTDI _{vol}	OTCM Dose per CTDI _{vol}	OTCM _{BP} Dose per CTDI _{vol}	OTCM _{BP} to ATCM difference (%)	OTCM to ATCM difference (%)	OTCM _{BP} to OTCM difference (%)
Small	1.1 ± 0.1	0.9 ± 0.1	0.7 ± 0.1	-31.4 ± 6.5*	-16.9 ± 4.1*	-17.3 ± 7.8*
Medium	1.0 ± 0.1	0.8 ± 0.1	0.6 ± 0.1	-36.8 ± 5.0*	-20.5 ± 4.3*	-20.4 ± 6.2*
Large	1.0 ± 0.1	0.8 ± 0.1	0.6 ± 0.1	-41.5 ± 5.4*	-20.6 ± 4.3*	-26.3 ± 5.0*
Breast dose						
Breast Size	ATCM Dose (mGy)	OTCM Dose (mGy)	OTCM _{BP} Dose (mGy)	OTCM _{BP} to ATCM difference (%)	OTCM to ATCM difference (%)	OTCM _{BP} to OTCM difference (%)
Small	8.0 ± 2.5	6.5 ± 1.8	5.4 ± 1.9	-32.6 ± 7.0*	-16.9 ± 4.1*	-18.7 ± 9.0*
Medium	9.3 ± 2.2	7.4 ± 1.6	5.8 ± 1.4	-38.3 ± 5.2*	-20.5 ± 4.3*	-22.3 ± 7.1*
Large	12.4 ± 2.1	9.8 ± 1.5	6.8 ± 1.5	-45.4 ± 7.7*	-20.6 ± 4.3*	-31.3 ± 8.7*

²Negative means dose reduction.

* represents statistical significant.

The breast dose saving of $OTCM_{BP}$ compared to ATCM was more significant for patients with larger breasts. For small (447 ± 187 g), medium (1068 ± 222 g), and large-sized (1929 ± 432 g) groups, the $OTCM_{BP}$ and ATCM h factors difference were $-31.4 \pm 6.5\%$, $-36.8 \pm 5.0\%$, and $-41.5 \pm 5.4\%$. The corresponding values in terms of breast dose were $32.6 \pm 7.0\%$, $38.3 \pm 5.2\%$, and $45.4 \pm 7.7\%$, respectively (Table 4). Compared to $OTCM$ alone, $OTCM_{BP}$ h factors decreased by $17.3 \pm 7.8\%$, $20.4 \pm 6.2\%$, and $26.3 \pm 5.0\%$ for small, medium, and large sized groups, respectively. The corresponding value in terms of breast dose were $18.7 \pm 9.0\%$, $22.3 \pm 7.1\%$, and $31.3 \pm 8.7\%$, respectively. The fitting coefficients of dose values vs. breast mass for the three protocols are given in Table 5 (Figure 7).

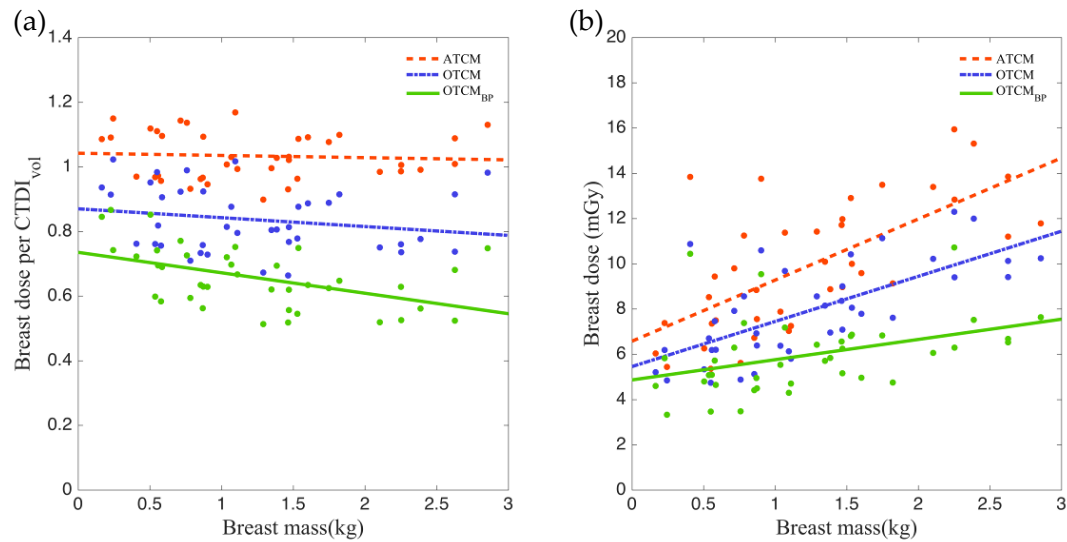


Figure 7: $CTDI_{vol}$ -normalized-breast dose coefficients linearly fitted to breast mass scanned with ATCM, OTCM and $OTCM_{BP}$ as equation (2).

Table 5: Fitting coefficients of breast dose fitted vs. breast mass.

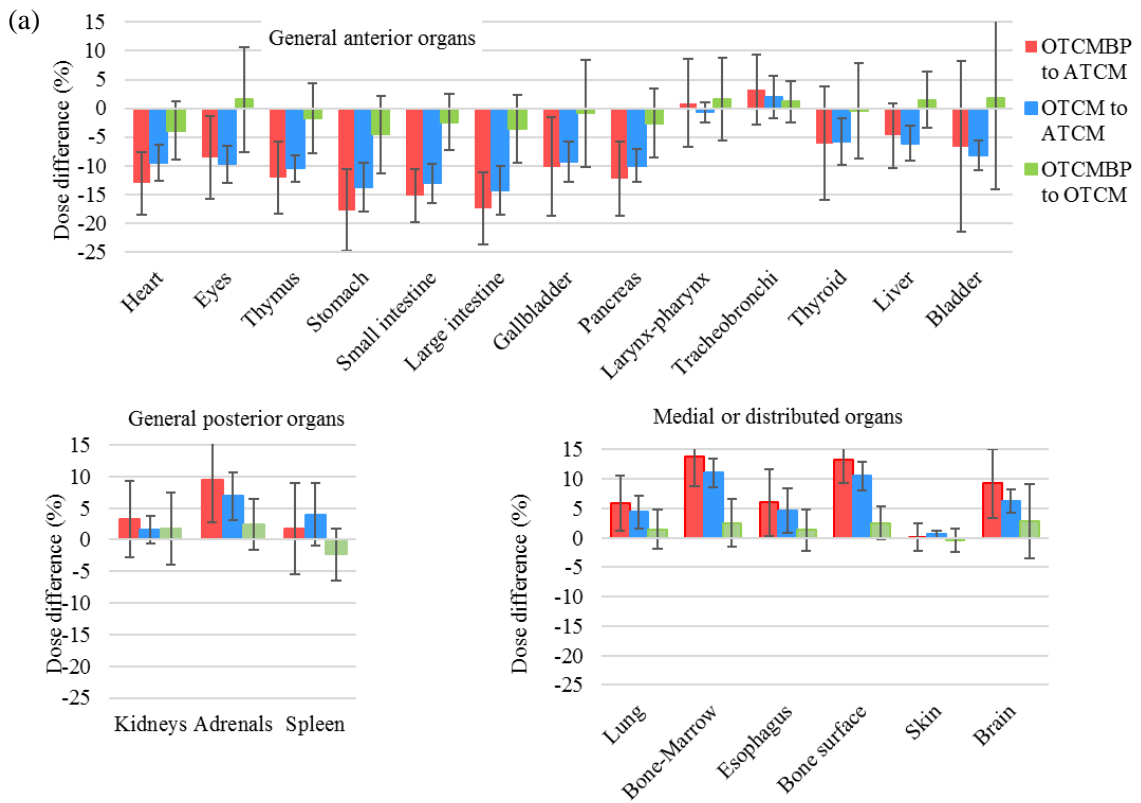
	CTDI _{vol} -normalized-breast dose coefficients			Breast dose		
	$p_{h,1}(kg^{-1})$	$p_{h,2}$	RMSE	$p_{D,1}(kg^{-1})$	$p_{D,2}$	RMSE
ATCM	-0.007	1.042	0.073	2.7	6.58	2.18
OTCM	-0.027	0.87	0.098	1.99	5.45	1.57
OTCM _{BP}	-0.063	0.735	0.085	0.89	4.86	1.57

3.2 Other organ dose

Besides breast, other radiosensitive organs exhibited dose differences in ATCM to OTCM, OTCM to OTCM_{BP}, and ATCM to OTCM_{BP} as in Figure 8. Compared to ATCM, OTCM significantly reduced dose to general anterior organs (except larynx-pharynx and tracheobronchi) ($p < 0.01$). Doses to several organs (thymus, stomach, small and large intestine, pancreases) decreased up to 10%. The doses to medial and posterior organ dose in OTCM compared to ATCM was increased by less than 10% ($p < 0.01$). For distributed organs of bone-marrow and bone-surface, which are located more towards posterior of the patient, organ doses were increased by 10%. The skin dose remained relatively constant. When using BP compared to OTCM alone, doses to anterior organs (heart, stomach, small and large intestine, pancreases) were decreased or not changed significantly. The doses to medial and posterior organs was increased by less than 3% or not significantly changed when using BP (except for spleen).

Figure 8 shows $CTDI_{vol}$ -normalized-dose fitted to patient chest diameter as an exponential function. For general anterior located organs, ATCM scan dose was higher than OTCM scan for all patients with various chest diameters, except for thyroid,

tracheo-bronchi and larynx-pharynx, whose doses from OTCM and/or OTCM_{BP} exceeds the doses from ATCM. The OTCM and OTCM_{BP} dose show few changes in coefficients. For medial or distributed organs and general posterior organs, the OTCM and OTCM_{BP} dose were generally larger than ATCM dose across all patient sizes, especially for larger sized patients, except for adrenal. The fitting parameters are in Table 7.



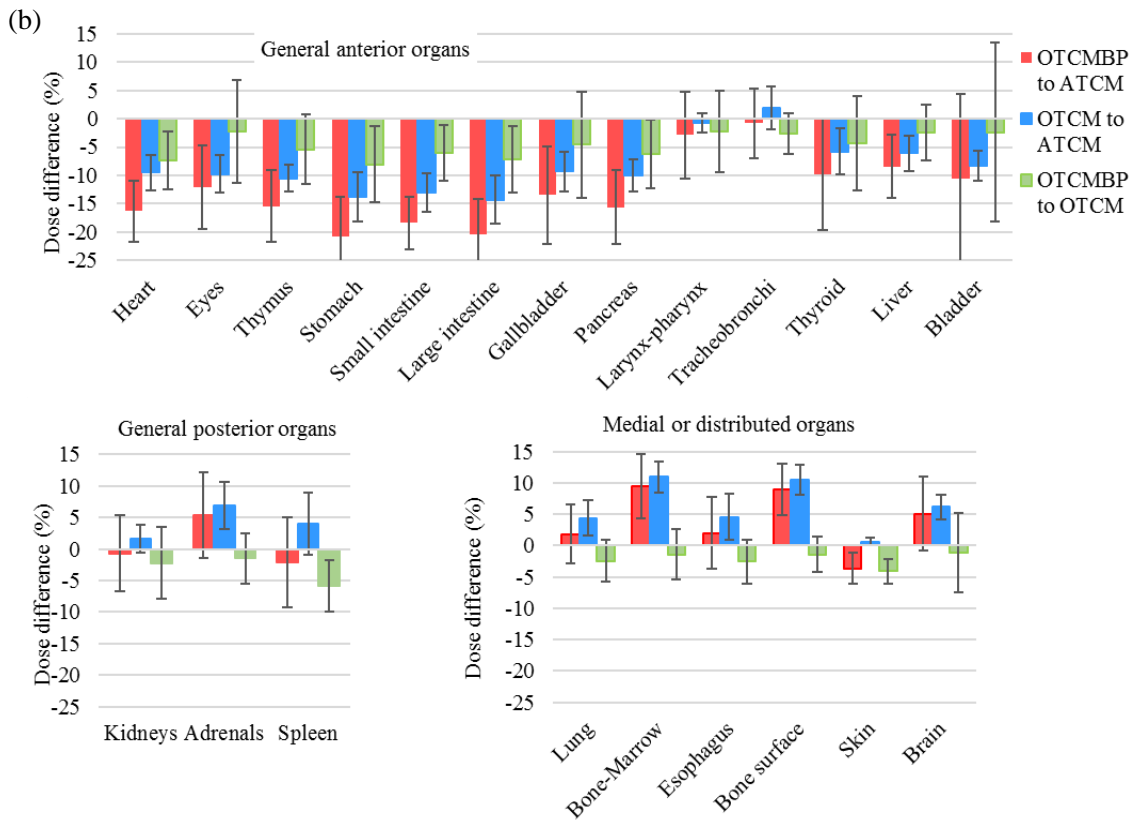
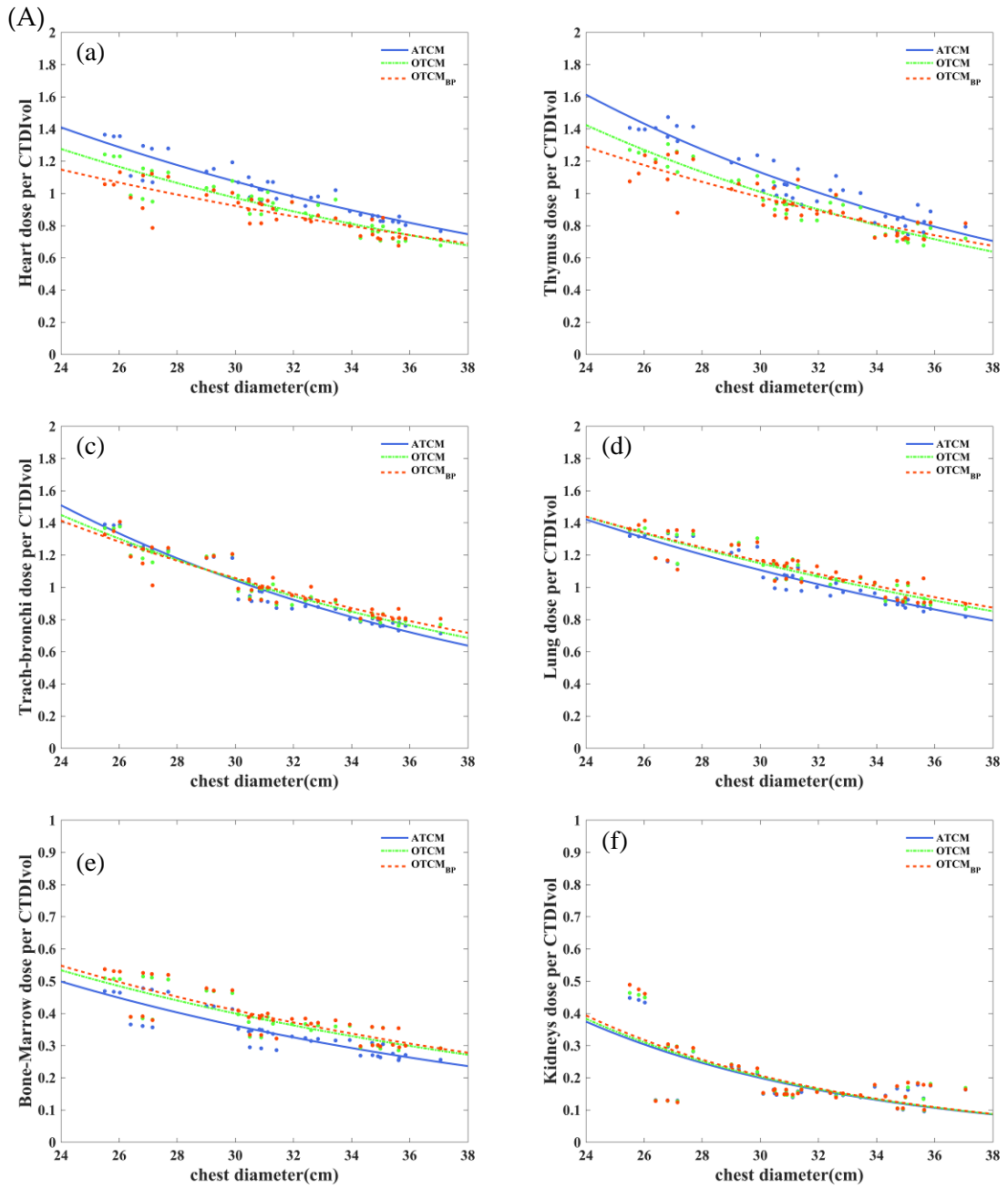


Figure 8: Differentiation for a) CTDI_{vol}-normalized-breast dose coefficients and b) breast dose across ATCM, OTCM and OTCM_{BP}.



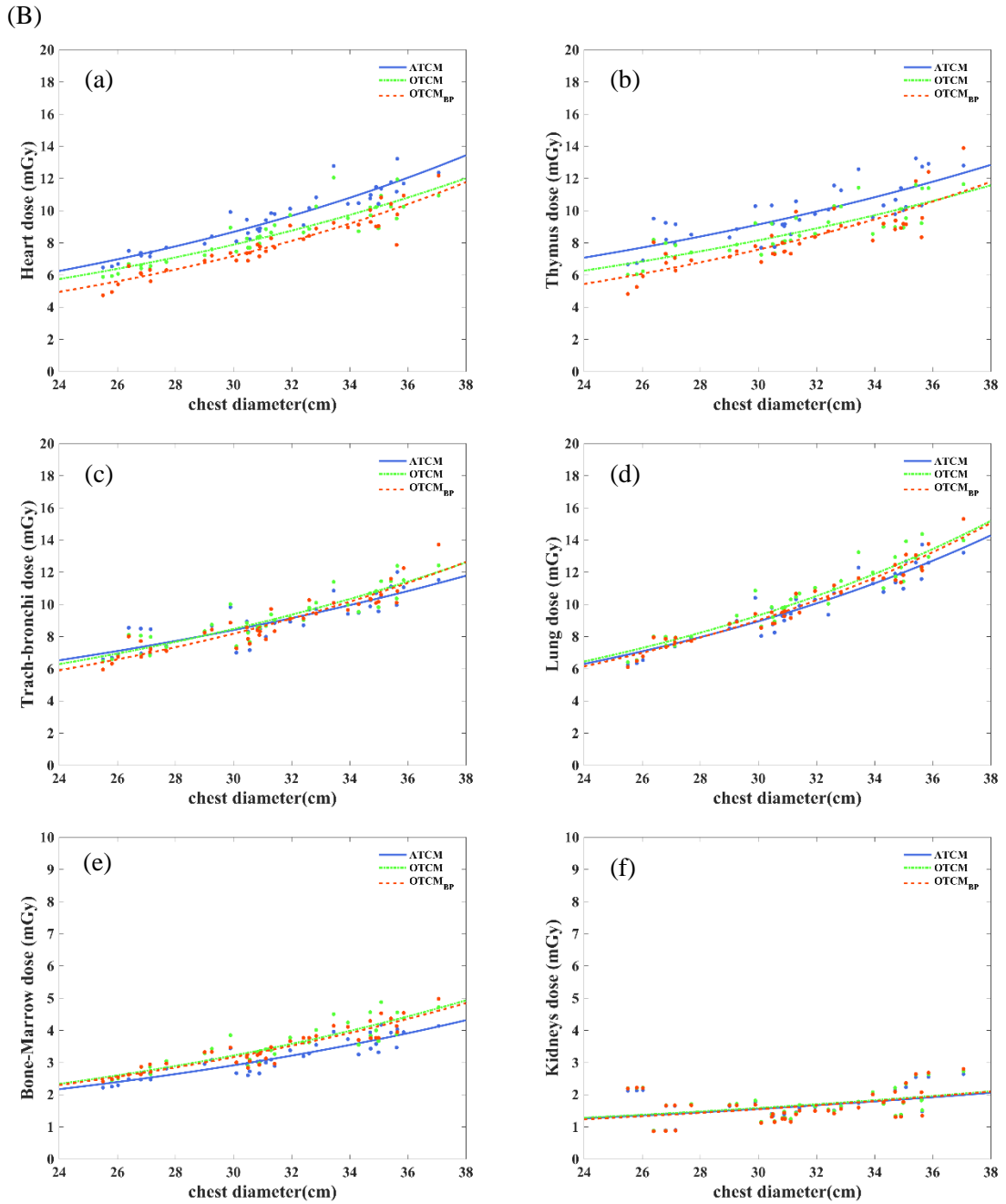


Figure 9: A) CTDI_{vol}-normalized-organ dose and B) organ dose fitted against model chest diameter as equation (1). Example organs from anterior (a), (b), and (c), medial and distributed (d) and (e), and posterior (f) group.

Table 6: Fitting parameters of organ dose v.s. chest diameter¹

CTDI _{vol} -normalized-organ dose vs. chest diameter fitting coefficients									
Organ	ATCM			OTCM			OTCM _{BP}		
	$\alpha_{h,ATCM}$	$\beta_{h,ATCM}$	R^2	$\alpha_{h,OTCM}$	$\beta_{h,OTCM}$	R^2	$\alpha_{h,OTCM,BP}$	$\beta_{h,OTCM,BP}$	R^2
Anterior organs									
Breast	-0.01	0.47	0.45	-0.03	0.65	0.56	-0.03	0.51	0.47
Heart	-0.05	1.43	0.86	-0.05	1.33	0.82	-0.04	1.01	0.71
Eyes	0.01	-4.55	0.09	0.00	-4.39	0.01	0.02	-4.75	0.13
Thymus	-0.06	1.90	0.89	-0.06	1.73	0.89	-0.05	1.37	0.75
Stomach	-0.05	1.05	0.31	-0.05	0.96	0.30	-0.04	0.51	0.21
Small intestine	0.03	-3.26	0.08	0.03	-3.24	0.06	0.03	-3.51	0.11
Large intestine	0.04	-3.43	0.12	0.03	-3.44	0.10	0.04	-3.67	0.14
Gallbladder	0.01	-2.17	0.02	0.01	-2.16	0.01	0.01	-2.13	0.01
Pancreas	-0.03	-0.32	0.09	-0.03	-0.45	0.09	-0.02	-0.69	0.06
Larynx-pharynx	-0.01	-1.09	0.09	-0.01	-1.18	0.06	0.00	-1.48	0.00
Trachea-bronchi	-0.06	1.89	0.94	-0.05	1.65	0.92	-0.05	1.51	0.86
Thyroid	-0.08	1.85	0.53	-0.07	1.51	0.53	-0.05	0.86	0.42
Liver	-0.03	0.36	0.46	-0.03	0.25	0.38	-0.03	0.16	0.29
Bladder	-0.01	-5.76	0.02	-0.01	-5.83	0.02	0.00	-6.07	0.00
Medial or distributed organs									
Lung	-0.04	1.35	0.87	-0.04	1.26	0.84	-0.04	1.22	0.79
Marrow (red)	-0.05	0.59	0.77	-0.05	0.53	0.72	-0.05	0.56	0.69
Esophagus	-0.06	1.69	0.94	-0.05	1.46	0.88	-0.05	1.38	0.83
Bone surface	-0.05	0.88	0.81	-0.04	0.83	0.77	-0.04	0.85	0.75
Skin	-0.04	-0.47	0.63	-0.04	-0.46	0.65	-0.04	-0.40	0.69
Brain	-0.01	-4.13	0.06	-0.01	-4.11	0.04	-0.01	-4.09	0.05
Posterior organs									
Kidneys	-0.11	1.54	0.48	-0.11	1.58	0.46	-0.11	1.64	0.45
Adrenals	-0.10	2.21	0.55	-0.10	2.48	0.54	-0.11	2.76	0.53
Spleen	-0.05	0.99	0.40	-0.04	0.83	0.29	-0.03	0.67	0.23

¹ The doses are fitted against chest diameter using exponential function as equation (1).

Organ dose v.s chest diameter fitting coefficients									
Organ	ATCM			OTCM			OTCM _{BP}		
	$\alpha_{D,ATCM}$	$\beta_{D,ATCM}$	R^2	$\alpha_{D,OTCM}$	$\beta_{D,OTCM}$	R^2	$\alpha_{D,OTCM,BP}$	$\beta_{D,OTCM,BP}$	R^2
Anterior organs									
Breast	0.09	-0.47	0.92	0.08	-0.32	0.83	0.07	-0.55	0.70
Heart	0.06	0.52	0.88	0.05	0.48	0.81	0.06	0.11	0.88
Eyes	0.13	-5.91	0.88	0.12	-5.72	0.87	0.13	-6.20	0.81
Thymus	0.04	0.93	0.64	0.04	0.78	0.69	0.06	0.37	0.68
Stomach	0.06	-0.18	0.40	0.06	-0.27	0.35	0.07	-0.72	0.40
Small intestine	0.13	-4.09	0.56	0.12	-4.00	0.54	0.14	-4.58	0.57
Large intestine	0.13	-3.92	0.59	0.12	-3.88	0.57	0.13	-4.37	0.58
Gallbladder	0.08	-2.10	0.42	0.08	-2.08	0.41	0.08	-2.08	0.38
Pancreas	0.09	-1.69	0.47	0.09	-1.77	0.48	0.09	-2.11	0.46
Larynx-pharynx	0.09	-2.04	0.76	0.09	-2.14	0.78	0.10	-2.41	0.80
Trachea-bronchi	0.04	0.86	0.75	0.05	0.65	0.84	0.05	0.47	0.86
Thyroid	0.03	0.89	0.15	0.04	0.49	0.30	0.05	-0.02	0.47
Liver	0.07	-0.45	0.83	0.07	-0.51	0.79	0.07	-0.61	0.79
Bladder	0.07	-6.12	0.33	0.07	-6.16	0.31	0.08	-6.54	0.37
Medial or distributed organs									
Lung	0.06	0.44	0.90	0.06	0.39	0.90	0.06	0.28	0.94
Marrow (red)	0.05	-0.41	0.81	0.05	-0.44	0.81	0.05	-0.45	0.85
Esophagus	0.05	0.64	0.83	0.06	0.44	0.87	0.06	0.34	0.91
Bone surface	0.05	-0.03	0.75	0.06	-0.07	0.79	0.06	-0.05	0.86
Skin	0.07	-1.51	0.89	0.07	-1.50	0.90	0.07	-1.49	0.90
Brain	0.10	-5.42	0.77	0.10	-5.43	0.74	0.10	-5.38	0.69
Posterior organs									
Kidneys	0.04	-0.61	0.16	0.04	-0.60	0.15	0.04	-0.71	0.15
Adrenals	0.03	0.60	0.16	0.02	0.78	0.11	0.02	0.89	0.06
Spleen	0.06	0.07	0.45	0.06	-0.08	0.46	0.07	-0.29	0.42

4. Discussion

Organ-based tube current modulation technique has been devised to minimize unnecessary radiation exposure to major radiosensitive organs while maintaining the required image quality. In this work, we evaluated the dose saving potential of an additional breast positioning technique for organ based TCM examinations. Compared to standard tube current modulation, organ-based tube current modulation offered an average of $19.3 \pm 4.5\%$ reduction in breast dose. Targeted breast positioning extended that reduction by an additive $21.3 \pm 7.3\%$. Targeted breast positioning takes a fuller advantage of OTCM for reducing breast dose in body CT examinations.

4.1 Organ-based tube current modulation and dose

In this study, a constant $CTDI_{vol}$ value was used for ATCM and OTCM scheme for each phantom. A previous study has argued that OTCM is less dose-economical compared to ATCM, and resulted in a 5 - 10% $CTDI_{vol}$ increase to maintain image quality¹⁴. When OTCM is utilized, the x-y modulation is shut off, the Z-plane mA is generated based on the average of AP and LAT attenuation. If techniques permit, keeping x-y plane modulation in OTCM would be more dose efficient. We simulated this scenario ($OTCM_{ideal}$), reducing mA_{ATCM} by 80% and a corresponding increase in the remaining projections. The dose reduction was larger in anterior organs. The dose for heart and thymus was reduced by $14.7 \pm 3.4\%$ and $20.0 \pm 4.6\%$, respectively. The dose

increase was smaller in distributed and posterior organs (except for spleen). No significant change was noted in lung, esophagus, and kidneys.

4.2 Compare with literature

4.2.1 Breast modeling

To take full advantage of OTCM, breast-positioning techniques constrain the breast to within the dose reduction zone. Seidenfuss *et al.* have demonstrated that a normal bra can constrain more breast tissue within the dose reduction zone³⁶. However, in that implementation, the breasts are still not fully sheltered, especially in women with larger breasts where only 83.3% of the volume is constrained. That study did not include the breast dose saving. In this study, we simulated the breast positioning technique that can optimize breast position beyond a normal bra's support by compressing more breast tissue to within the dose reduction zone. To ensure the modeled breast locations reflect real scenario, the percentage of breast tissue within the dose reduction zone was compared with those reported in literature. Seidenfuss *et al.* reported breast volumes within dose reduction zone on CT images from 578 female patients with and without brassiere³⁶. On average, $60.4 \pm 24.7\%$ and $91.3 \pm 9.4\%$ of breast volume was within dose reduction zone with and without a brassiere, respectively³⁶. In our work, the average breast tissue within the dose reduction zone was $64.6 \pm 15.2\%$ originally, and increased to $93.8 \pm 4.0\%$ after applying BP. The ratio of breast within the dose reduction zone is

higher in our study compared to Seidenfuss *et al.* because in our technique, we compressed the breast tissue closer towards the center of the torso.

4.2.2 Dose savings

The breast dose savings of OTCM and OTCM_{BP} from ATCM were compared with physical phantoms. Comparing OTCM to ATCM on an anthropomorphic phantom with breast attachment Lungren *et al.* showed that with 37% reduced dose on average, the anterior and posterior breast dose reduction ranges from 29-45% and 9-19%, respectively, ¹⁶. Our results were generally consistent; with OTCM, the average breast dose reduction ranges were 11.0% to 28.7%. For ATCM to OTCM_{BP}, the breast dose was reduced from 20.6% to 48.1% when normalized to CTDI_{vol}, and 21.0% to 54.8% without normalization. Another study reported that breast dose was reduced by 34%, 34%, and 39% with OTCM compared to ATCM for small, medium, and large semi-anthropomorphic phantoms (30×20, 35×25, 40×30 cm in lateral and posterior-anterior dimension)¹⁴. To derive breast dose corresponding to the above average chest diameter in our study, the breast dose was fitted to chest diameter as an exponential function (Figure 8). On average, compared to ATCM, OTCM reduced *h* factor by 12.7%, 18.0%, and 23.0%, and breast dose by 13.1%, 18.1%, and 22.8%. The OTCM savings in our study was smaller compared to the literature, as the XCAT breasts were explicitly modeled, while the phantoms used in other studies were with “underdeveloped” breasts (i.e., the

breasts were not spread) ^{6, 13, 14, 16, 37}. Thus, more lateral portions of the XCAT breasts were in the dose-increased zone. The full advantage of OTCM was not taken without BP. The OTCM_{BP} saved h factor by 30.01%, 35.33%, and 40.25%, and breast dose by 33.8%, 38.1%, 42.1% for phantoms with 25 cm, 30 cm, and 35 cm chest diameter, respectively.

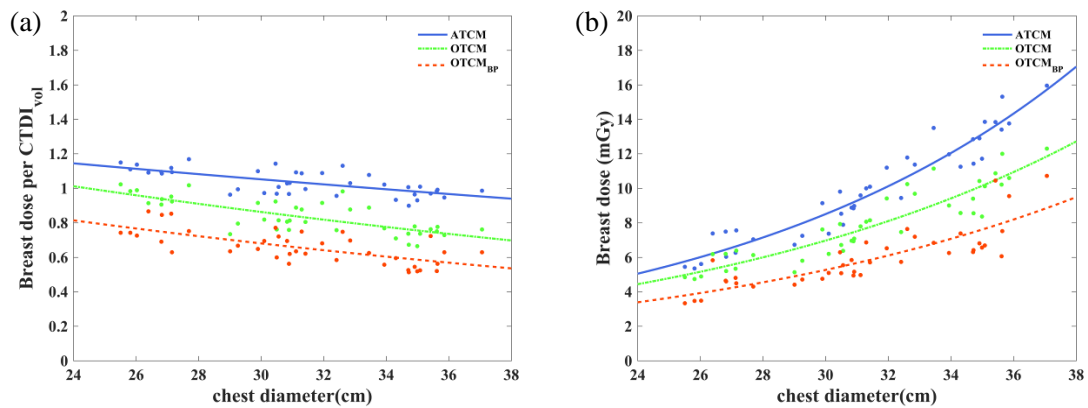


Figure 10: a) CTDI_{vol}-normalized-breast dose coefficients and b) breast dose linearly fitted to breast mass scanned with ATCM, OTCM and OTCM_{BP} as equation (2).

Other organ doses were also compared with physical phantoms. Lungren et al. has reported anterior organ dose reduced 17-47%; posterior organ dose significantly increased; lateral and inner organ dose showed similar results ¹⁶. Our results were consistent on some typical anterior and posterior organs. Thymus and kidney dose changed by 10.5% and -1.6% (8.4% and -1% from Lungren *et al.*). The skin dose profile was also compared with measurement of physical phantoms from the literature. The skin dose was sampled and interpolated within 360 degrees for each phantom on one

selected slice. The slice was chosen to contain a large volume of breast tissue. The interpolated skin dose was further averaged across all phantoms. Duan *et al.* reported surface dose of anthropomorphic phantoms receiving OTCM and fixed mA scan (mA_{fix})¹³. To compare our results to those of Duan *et al.*, the dose from each our protocols was normalized by CTDI_{vol} and scaled to unit mA on average. Our results showed excellent agreement with the measurement from physical phantoms (Figure 10). For OTCM, the dose was unsymmetrical on left and right reduction zone, which is due to unequal upward and downward transition times. Compared to mA_{fix} , the mA_{ATCM} is generally larger in LAT and smaller in AP.

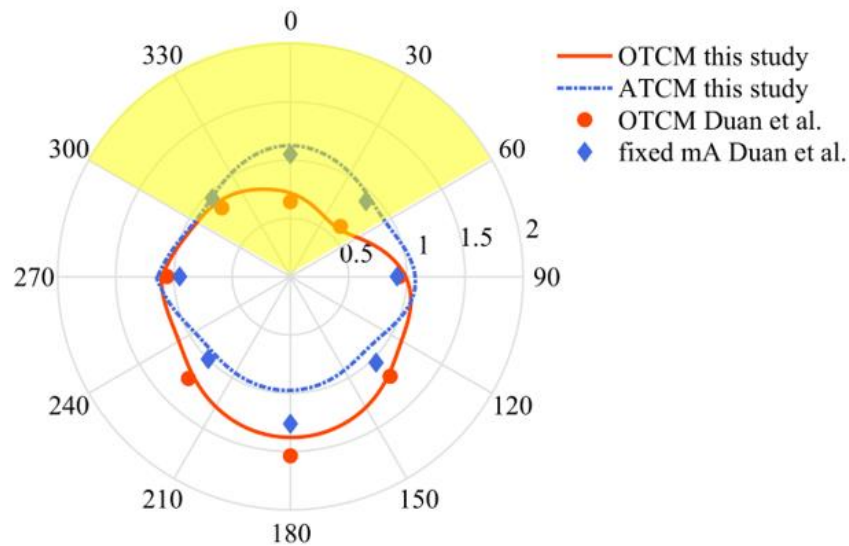


Figure 11: Skin dose from ATCM and OTCM in computerized phantom for this study compared with Duan *et al.* measured with physical phantoms with OTCM and fixed mA. The dose was averaged to a unit mean for comparisons. For this study, skin dose profile was averaged across all phantoms. The dose reduction zone is shaded in yellow.

4.3 Breast positioning technique advantage

Although use of a patient's own brassiere is cost efficient, a specially designed BP support would be superior as it compresses more of the breast tissue within the dose reduction zone, especially the outer quadrant of the breast, which more than half of breast carcinoma occurs^{18, 19,38}. With a normal brassiere, 17% of the breast is outside the dose reduction zone for large sized breasts³⁶. With the implemented BP, the portion of breast tissue within the dose increased zone decreases to 6%. Furthermore, BP constrains an average constant portion (94%) of breast tissue within the dose reduction zone in all groups. However, normal brassieres performance varies among different breast-size groups³⁶. The dose savings effect and potential artifacts in CT images with various normal brassieres is yet to be examined. A standardized BP allows one to accurately monitor dose and prospectively optimize CT procedure.

4.5 Limitations

This work has several limitations. First, the dose coefficient estimation was limited to one CT scanner. Second, although the dose reduction potential was demonstrated, an optimized positioning technique with minimum dose and patient comfort is yet to be defined. For each phantom, only one breast positioning was simulated. Third, image quality was not examined in this study. In previous studies, no significant difference in noise and CT numbers have been reported when comparing

OTCM with ATCM or fixed mA scans using physical phantoms^{13, 14, 16}. Neither were streaking and beam hardening artifacts with perceivable differences found. In Seidenfuss *et al.* work, the image quality was assessed for women scanned with OTCM CT, with and without a normal brassiere; no artifacts were reported³⁶. A similar study will be conducted for OTCM_{BP} in the future.

5. Conclusion

In this study, the dose reduction potential of alternate breast positioning was evaluated for organ-based TCM examinations. Keeping $CTDI_{vol}$ constant, on average, compared to ATCM, OTCM reduced the breast dose by ~20%. The average breast dose was further decreased by an additional 21% with targeted breast positioning. Targeted breast positioning is needed to take full advantage of OTCM for reducing breast dose in body CT examinations.

References

- 1 IMV, "CT Market Outlook Report," 2014).
- 2 R.G. Evens, F. Mettler, "National CT use and radiation exposure: United States 1983," *American journal of roentgenology* **144**, 1077-1081 (1985).
- 3 D.J. Brenner, E.J. Hall, "Computed Tomography — An Increasing Source of Radiation Exposure," *New England Journal of Medicine* **357**, 2277-2284 (2007).
- 4 C.H. McCollough, G.H. Chen, W. Kalender, S. Leng, E. Samei, K. Taguchi, G. Wang, L. Yu, R.I. Pettigrew, "Achieving routine submillisievert CT scanning: report from the summit on management of radiation dose in CT," *Radiology* **264**, 567-580 (2012).
- 5 S.V. Vollmar, W.A. Kalender, "Reduction of dose to the female breast in thoracic CT: a comparison of standard-protocol, bismuth-shielded, partial and tube-current-modulated CT examinations," *European radiology* **18**, 1674-1682 (2008).
- 6 J. Wang, X. Duan, J.A. Christner, S. Leng, K.L. Grant, C.H. McCollough, "Bismuth shielding, organ-based tube current modulation, and global reduction of tube current for dose reduction to the eye at head CT," *Radiology* **262**, 191-198 (2012).
- 7 J. Valentin, *The 2007 recommendations of the international commission on radiological protection*. (Elsevier Oxford, 2007).
- 8 E. Angel, N. Yaghmai, C.M. Jude, J.J. DeMarco, C.H. Cagnon, J.G. Goldin, C.H. McCollough, A.N. Primak, D.D. Cody, D.M. Stevens, "Dose to radiosensitive organs during routine chest CT: effects of tube current modulation," *AJR. American journal of roentgenology* **193**, 1340 (2009).
- 9 B.L. Fricke, L.F. Donnelly, D.P. Frush, T. Yoshizumi, V. Varchena, S.A. Poe, J. Lucaya, "In-plane bismuth breast shields for pediatric CT: effects on radiation dose and image quality using experimental and clinical data," *American Journal of Roentgenology* **180**, 407-411 (2003).
- 10 D. McLaughlin, R. Mooney, "Dose reduction to radiosensitive tissues in CT. Do commercially available shields meet the users' needs?," *Clinical radiology* **59**, 446-450 (2004).
- 11 T. Kubo, P.-J.P. Lin, W. Stiller, M. Takahashi, H.-U. Kauczor, Y. Ohno, H. Hatabu, "Radiation dose reduction in chest CT: a review," *American journal of roentgenology* **190**, 335-343 (2008).
- 12 M. Raissaki, K. Perisinakis, J. Damilakis, N. Gourtsoyiannis, "Eye-lens bismuth shielding in paediatric head CT: artefact evaluation and reduction," *Pediatric radiology* **40**, 1748-1754 (2010).
- 13 X. Duan, J. Wang, J.A. Christner, S. Leng, K.L. Grant, C.H. McCollough, "Dose reduction to anterior surfaces with organ-based tube-current modulation:

- evaluation of performance in a phantom study," *American Journal of Roentgenology* **197**, 689-695 (2011).
- 14 J. Wang, X. Duan, J.A. Christner, S. Leng, L. Yu, C.H. McCollough, "Radiation dose reduction to the breast in thoracic CT: comparison of bismuth shielding, organ-based tube current modulation, and use of a globally decreased tube current," *Medical physics* **38**, 6084-6092 (2011).
- 15 E. Samei, "Pros and cons of organ shielding for CT imaging," *Pediatric radiology* **44**, 495-500 (2014).
- 16 M.P. Lungren, T.T. Yoshizumi, S.M. Brady, G. Toncheva, C. Anderson-Evans, C. Lowry, X.R. Zhou, D. Frush, L.M. Hurwitz, "Radiation dose estimations to the thorax using organ-based dose modulation," *American Journal of Roentgenology* **199**, W65-W73 (2012).
- 17 S. Taylor, D.E. Litmanovich, M. Shahrzad, A.A. Bankier, P.A. Gevenois, D. Tack, "Organ-based Tube Current Modulation: Are Women's Breasts Positioned in the Reduced-Dose Zone?," *Radiology* **274**, 260-266 (2014).
- 18 A.H.S. Lee, "Why is carcinoma of the breast more frequent in the upper outer quadrant? A case series based on needle core biopsy diagnoses.," *The Breast* **14**, 2 (2005).
- 19 K.J. Hurt, M.W. Guile, J.L. Bienstock, H.E. Fox, E.E. Wallach, *The Johns Hopkins manual of gynecology and obstetrics*. (Lippincott Williams & Wilkins, 2012).
- 20 W.P. Segars, J. Bond, J. Frush, S. Hon, C. Eckersley, C.H. Williams, J. Feng, D.J. Tward, J.T. Ratnanather, M.I. Miller, D. Frush, E. Samei, "Population of anatomically variable 4D XCAT adult phantoms for imaging research and optimization," *Medical Physics* **40**, 043701 (2013).
- 21 W. Segars, M. Mahesh, T. Beck, E. Frey, B. Tsui, "Realistic CT simulation using the 4D XCAT phantom," *Medical physics* **35**, 3800-3808 (2008).
- 22 W. Segars, G. Sturgeon, S. Mendonca, J. Grimes, B.M. Tsui, "4D XCAT phantom for multimodality imaging research," *Medical physics* **37**, 4902-4915 (2010).
- 23 J. Valentin, "Basic anatomical and physiological data for use in radiological protection: reference values: ICRP Publication 89," *Annals of the ICRP* **32**, 1-277 (2002).
- 24 X. Li, W.P. Segars, E. Samei, "The impact on CT dose of the variability in tube current modulation technology: a theoretical investigation," *Physics in medicine and biology* **59**, 4525 (2014).
- 25 M. Yaffe, J. Boone, N. Packard, O. Alonzo-Proulx, S.-Y. Huang, C. Peressotti, A. Al-Mayah, K. Brock, "The myth of the 50-50 breast," *Medical physics* **36**, 5437-5443 (2009).

- 26 G. Richard Hammerstein, D.W. Miller, D.R. White, M. Ellen Masterson, H.Q. Woodard, J.S. Laughlin, "Absorbed Radiation Dose in Mammography 1," *radiology* **130**, 485-491 (1979).
- 27 X. Li, E. Samei, W.P. Segars, G.M. Sturgeon, J.G. Colsher, G. Toncheva, T.T. Yoshizumi, D.P. Frush, "Patient-specific radiation dose and cancer risk estimation in CT: Part I. Development and validation of a Monte Carlo program," *Medical physics* **38**, 397-407 (2011).
- 28 S.A. Maas, B.J. Ellis, G.A. Ateshian, J.A. Weiss, "FEBio: finite elements for biomechanics," *Journal of biomechanical engineering* **134**, 011005 (2012).
- 29 X. Li, E. Samei, W.P. Segars, G.M. Sturgeon, J.G. Colsher, G. Toncheva, T.T. Yoshizumi, D.P. Frush, "Patient-specific radiation dose and cancer risk estimation in CT: part II. Application to patients," *Medical physics* **38**, 408-419 (2011).
- 30 J. Baro, J. Sempau, J. Fernández-Varea, F. Salvat, "PENELOPE: an algorithm for Monte Carlo simulation of the penetration and energy loss of electrons and positrons in matter," *Nuclear Instruments and Methods in Physics Research Section B: Beam Interactions with Materials and Atoms* **100**, 31-46 (1995).
- 31 J. Sempau, J. Fernandez-Varea, E. Acosta, F. Salvat, "Experimental benchmarks of the Monte Carlo code PENELOPE," *Nuclear Instruments and Methods in Physics Research Section B: Beam Interactions with Materials and Atoms* **207**, 107-123 (2003).
- 32 X. Tian, X. Li, W.P. Segars, D. Frush, E. Samei, presented at the SPIE Medical Imaging2014 (unpublished).
- 33 X. Tian, X. Li, W.P. Segars, D.P. Frush, E. Samei, "Prospective estimation of organ dose in CT under tube current modulation," *Medical physics* **42**, 1575-1585 (2015).
- 34 X. Li, E. Samei, W.P. Segars, G.M. Sturgeon, J.G. Colsher, D.P. Frush, "Patient-specific radiation dose and cancer risk for pediatric chest CT," *Radiology* **259**, 862-874 (2011).
- 35 A.C. Turner, D. Zhang, M. Khatonabadi, M. Zankl, J.J. DeMarco, C.H. Cagnon, D.D. Cody, D.M. Stevens, C.H. McCollough, M.F. McNitt-Gray, "The feasibility of patient size-corrected, scanner-independent organ dose estimates for abdominal CT exams," *Medical physics* **38**, 820-829 (2011).
- 36 A. Seidenfuss, A. Mayr, M. Schmid, M. Uder, M.M. Lell, "Dose Reduction of the Female Breast in Chest CT," *American Journal of Roentgenology* **202**, W447-W452 (2014).
- 37 B.J. O'Hea, A.D. Hill, A.M. El-Shirbiny, S.D. Yeh, P.P. Rosen, D.G. Coit, P.I. Borgen, H.S. Cody, "Sentinel lymph node biopsy in breast cancer: initial

experience at Memorial Sloan-Kettering Cancer Center," *Journal of the American College of Surgeons* **186**, 423-427 (1998).

³⁸ P.D. Darbre, "Recorded quadrant incidence of female breast cancer in Great Britain suggests a disproportionate increase in the upper outer quadrant of the breast," *Anticancer research* **25**, 2543-2550 (2005).